IOPscience iopscience.iop.org

Home Search Collections Journals About Contact us My IOPscience

Structural characterization and refractive index dispersion analysis of HgSe thin films grown by reactive solutions

This article has been downloaded from IOPscience. Please scroll down to see the full text article.

2007 J. Phys.: Condens. Matter 19 116213

(http://iopscience.iop.org/0953-8984/19/11/116213)

View the table of contents for this issue, or go to the journal homepage for more

Download details:
IP Address: 129.252.86.83
The article was downloaded on 28/05/2010 at 16:36

Please note that terms and conditions apply.

J. Phys.: Condens. Matter **19** (2007) 116213 (11pp) doi:10.1088/0953-8984/19/11/116213

Structural characterization and refractive index dispersion analysis of HgSe thin films grown by reactive solutions

S Y Girgis, A M Salem[1] and M S Selim

Physics Division, Electron Microscopy and Thin Films Department, National Research Center, Cairo, Egypt

E-mail: salemar55@hotmail.com

Received 16 May 2006, in final form 5 February 2007
Published 5 March 2007
Online at stacks.iop.org/JPhysCM/19/116213

Abstract
Reproducible and good quality HgSe thin films can be grown at room temperature on microscopic glass substrates using the reactive solutions process. The x-ray diffraction patterns for the as-grown films, as well as those for the precipitated powder collected from the bath at the end of the chemical reaction, revealed a polycrystalline structure corresponding to the cubic phase. The surface topography and the elemental chemical composition of HgSe thin films grown on a carbon stub were investigated using scanning electron microscopy. The optical properties of HgSe thin films grown onto glass substrates were investigated from the recorded transmission and reflection data in the wavelength range 700–2500 nm. The refractive index dispersion of the as-grown films was characterized on the basis of simple dispersion theory, from which the average oscillator position, λ_o, average oscillator strength, S_o, and the high frequency dielectric constant, ε_∞, were calculated. Graphical representations of the surface and volume energy loss functions were also presented.

1. Introduction

Recently, chalcogenide thin films of different metals have attracted much attention due to their potential applications in solar selective coatings, solar cells, sensors, photoconductors, etc. Thin films of metal chalcogenide can be deposited on glass, metal, and other substrates by a variety of techniques such as vacuum evaporation, sputtering, chemical vapour deposition, spray pyrolysis, and reactive solutions growth (RSG). Of these, there is no doubt that RSG is the simplest and most economical method. RSG is a technique in which thin films are deposited on substrates immersed in dilute solutions containing metal ions and sulfide or selenide ions.

[1] Author to whom any correspondence should be addressed.

 © 2007 IOP Publishing Ltd Printed in the UK

This process usually uses a chelating agent to control the release of metal ions and sulfide ions to produce the controlled homogeneous precipitation of the film on the solid substrate. RSG is well suited for producing large area thin films and has many advantages [1–6]: it does not require sophisticated instruments like vacuum system and other expensive equipment and the starting chemicals are commonly available and cheap; the low temperature deposition avoids oxidation and corrosion of metallic substrates and various substrates including insulators, semiconductors or metals can be used; the preparation parameters are easily controlled.

HgSe is a member of the II–VI group. In the last few years, a lot of attention has been diverted towards the use of ternary alloy/solid solution thin films containing HgSe as a host material in optoelectronic applications including photoconductive photovoltaic, IR detector, IR emitter, tunable lasers and thermoelectric coolers [7–9]. Consequently, many studies have been carried out to investigate the structural properties of HgSe materials [10–12]. Some investigations also reported that HgSe thin films have direct optical transition with a band gap estimated from the absorption spectrum of energy 0.8 eV [11]. However, to the best of our knowledge there is no literature data available on the refractive index of HgSe thin films. Accurate knowledge of the refractive index of HgSe thin films is crucial to provide the precision required for optoelectronic applications and in the design of integrated optical devices.

The present work reports the deposition of HgSe thin films grown via reactive solutions. The structural characterization as well as the refractive index dispersion analysis of as-grown HgSe thin films is presented in detail.

2. Experimental details

2.1. Substrate cleaning

Substrate cleaning plays an important role in the deposition of thin films. Well cleaned substrates are required for the deposition of thin films, since a contaminated substrate surface provides nucleation sites facilitating the growth which results in non-uniform film growth. The glass substrates were boiled in 1 M chromic acid for 2 h, and rinsed in double distilled water. Thereafter, the substrates were dried in air, and weighed on a microbalance.

2.2. Growth of HgSe thin film

HgSe thin films were grown onto pre-cleaned glass substrates from a solution containing soluble complexes of mercury and selenosulfate ions. The proposed route is based on a hydrolysis of selenosulfate to selenide anions in alkaline solution and slow dissociation of the complexed ions. The following stock solutions were prepared to deposit HgSe thin films: 5 g of HgO was dissolved in 25 ml formamide solution with constant stirring for about $1\frac{1}{2}$ h. The resulting clear solution was made up to 250 ml with double distilled water and used as a stock solution for Hg^{2+} ions. Sodium selenosulfate solution was prepared by dissolving elemental selenium powder (5 g) in a sodium sulfite solution; prepared by mixing 12 g of anhydrous sodium sulphite in 100 ml of double distilled water. The mixture was then refluxed for 8 h. The little unreacted selenium powder precipitated in the prepared solution at the end of the chemical reaction was filtered off and the resultant solution was stored in a dark bottle. It is recommended that selenosulfate stock solution is used within 2–5 days. The chemicals used were all of analytical grade.

For the deposition of HgSe thin films, 8 ml of freshly prepared Hg^{2+} solution was taken in a beaker to which 6.5 ml of 2 M NaOH solution was added with constant stirring followed by 2.2 ml of 0.2 M sodium selenosulfate. The resulting solution was made up to 25 ml with

double distilled water. The resulting mixture was stirred for a few seconds. The pH value of the final solution should be about 10.5. The pre-cleaned glass substrates were supported almost vertically at room temperature into the final solution without stirring. The solution gradually turned black. Substrates were taken out at different durations: 2, 2.5, 3 h. Black uniform and strongly adherent films were coated on both sides of the substrates. The adhesion of the deposited films was tested by subjecting the as-grown films to a steady stream of distilled water. The film on one side of the substrate was removed using cotton swabs moistened with diluted HCl, while the other side was used for the experimental investigations. A black precipitation powder collected from the bath as a result of the reaction was washed well several times with double distilled water and dried, until a constant weight was attained. The basic chemical reaction leads to the formation HgSe thin films via the reactive solutions; the growth of HgSe thin films is discussed in [13].

2.3. Characterization of HgSe thin films

X-ray diffraction, (XRD) of Ni-filtered Cu Kα radiation (Type Philips PW 1373, operating at 40 kV and 25 mA) was used to examine the structure of both the as-grown films and the precipitated powder collected from the bath. X-ray scanning was performed along the entire 2θ range from 10° to 80°, to detect all the possible diffraction peaks. A scanning electron microscope, (SEM), (Type JEOL-JSM-T 200) interfaced with an energy dispersive x-ray unit (EDX) operating at 25 kV was employed to investigate the surface topography and the elemental chemical composition of the as-grown films.

A double beam spectrophotometer, with automatic computer data acquisition, (Type Jasco, V-570, Rerll-00, UV–visible–NIR) with photometric accuracy of ± 0.002–0.004 absorbance and $\pm 0.3\%$ transmittance was employed to record the optical transmission and reflection spectra of the deposited films over the wavelength range 700–2500 nm, at normal light incidence. A clean glass substrate identical to that coated with HgSe film was used as a reference to record the absolute transmission of the deposited film. On the other hand the measurements were made in various parts of the deposited films, scanning the entire sample, and a very good reproduction of spectra was generally achieved. The thicknesses of the deposited films were determined by the weight difference method, in which the area and weight of the deposited films were determined. All structural and optical measurements reported in the present work were performed at room temperature.

3. Results and discussion

3.1. Structural characterization of HgSe thin films

The comparative patterns of the x-ray diffraction for the as-grown HgSe films, of thickness 418 and 597 nm, respectively, and that obtained for precipitated powder collected from the bath are shown in figures 1(a) and (b). The patterns show polycrystalline structure. The calculated plane-spacing '*d*' values for such samples agree quit well with the standard XRD data for HgSe cubic phase[1]. The calculated '*d*' values from XRD patterns of the as-grown HgSe films and those values for the precipitated powder collected from the bath in comparison with the corresponding values of standard XRD data for HgSe are summarized in table 1. The satisfactory agreement among the '*d*' values confirms the presence of HgSe cubic phase with lattice constant, $a = 0.6087$ nm. A typical energy dispersive x-ray spectrum of an as-grown film of thickness 418 nm is shown in figure 2. The figure was used to find the percentage

[1] JCPDS, Card No: 8-469.

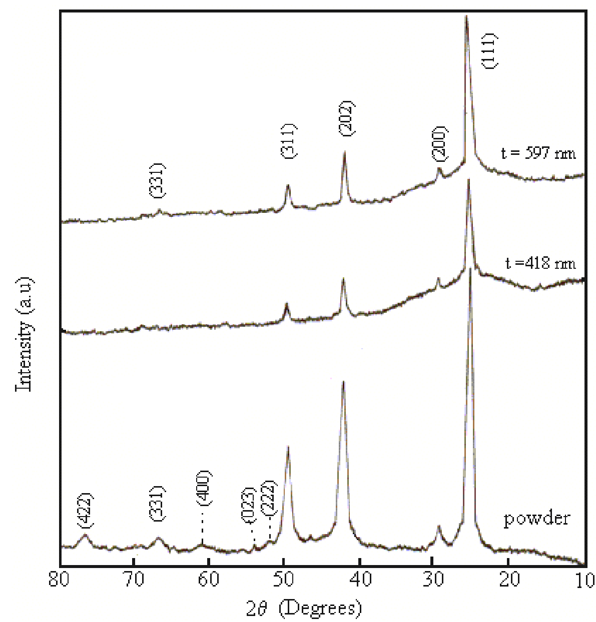

Figure 1. X-ray diffraction pattern of chemically deposited HgSe thin films.

Table 1. X-ray diffraction data of chemically deposited HgSe films.

		d values		
Powder	Film $t = 418$ nm	Film $t = 597$ nm	Stand. Card No:8-469	*hkl*
3.511	3.509	3.513	3.510	111
3.041	3.017	3.018	3.041	200
2.131	2.130	3.135	2.151	220
1.827	1.824	1.827	1.835	311
1.739	—	—	1.757	222
1.683	—	—	—	023
1.517	—	—	1.521	400
1.389	—	1.391	1.396	331
1.235	—	—	1.242	422

of the elemental chemical composition of as-grown HgSe film (see the inset of figure 2). It was found that the at.% of as-grown films is 46.73:45.07:08.22 corresponding to Hg:Se:K, respectively. The presence of K element may be attributed to an impurity either from the source materials or from the carbon stub. Hence, the chemical composition of the investigated sample can be re-written in the form $Hg_{0.986}Se_{0.95}K_{0.064}$, indicating that the as-grown films are nearly stoichiometric. It is seen from the scanning electron micrograph, figure 2(b), that the as-grown HgSe films show islands formed from aggregate spherical particles in a heterogeneous size.

3.2. Refractive index dispersion and optical band gap

Figure 3 shows the transmittance, T, and reflectance, R, spectra of three typical representative HgSe thin films as a function of wavelength and with different film thickness. The observed

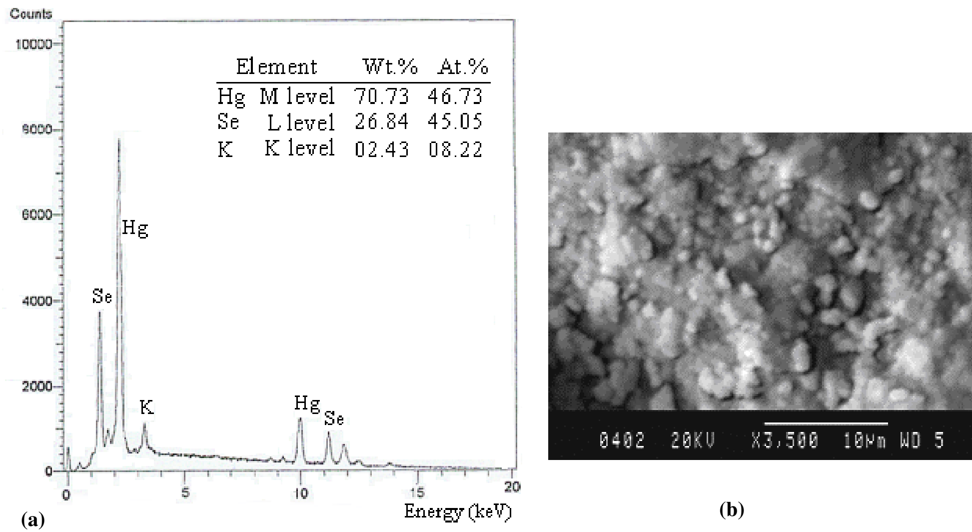

Figure 2. (a) The EDX spectra of an HgSe thin film deposited on a carbon stub. (b) The corresponding surface morphology.

transmittance spectra of HgSe thin films demonstrate that the as-grown films was highly transparent (>85%) in the near infrared region, indicating a fairly smooth surface and relatively good homogeneity of as-grown HgSe films, which is consistent with the results of the SEM. It was also observed that the as-grown films have an absorption edge extended from 700 nm up to nearly 1500 nm. With increasing film thickness the transmittance decreases uniformly with wavelength, and in the wavelength range of about 1500–2500 nm, the transmittance increases as the reflectance decreases. In the near infrared (NIR) spectral region $T + R \approx 1$ indicates that almost no scattering or absorption occur.

Following the analysis given by Pankove [14], the transmission in the absence of interference fringes of a thin film deposited on a perfectly smooth substrate is given by:

$$T = \frac{[(1 - R)^2 \exp(-\alpha t)]}{[1 - R^2 \exp(-2\alpha t)]}, \tag{1}$$

where t is the film thickness and α is the absorption coefficient ($\alpha = 4\pi\kappa/\lambda$).

For normal light incidence, the reflectivity, R may be expressed in terms of the real refractive index, n, and the extinction coefficient, k, by

$$R = \frac{(n - 1)^2 + k^2}{(n + 1)^2 + k^2}. \tag{2}$$

Solving equation (2) for n gives

$$n = \frac{(1 + R) + \sqrt{4R - (1 - R)^2 k^2}}{1 - R}. \tag{3}$$

Figure 4 shows the spectral variation of the refractive index, n, and extinction coefficient, k, versus wavelength, λ. It is obvious that a slight variation is observed for both n and k with the film thickness. The vertical bars illustrate the spread in both values for the given film thickness. Both n and k values were decreased with increasing wavelength. Namely, the refractive index decreases from a value of 2.618 at $\lambda = 1550$ nm reaching a value of $n = 2.578$ at $\lambda = 2500$ nm.

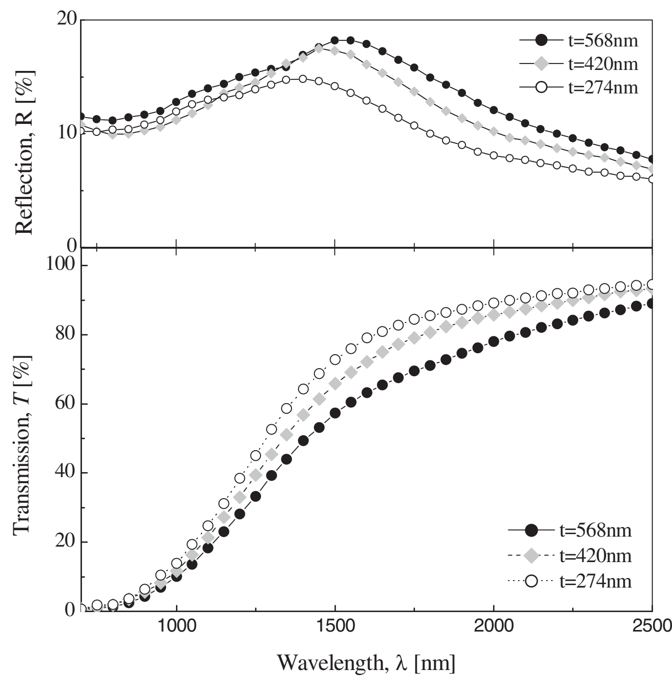

Figure 3. The optical transmittance and reflectance spectra of HgSe thin films for three typical representative different film thicknesses.

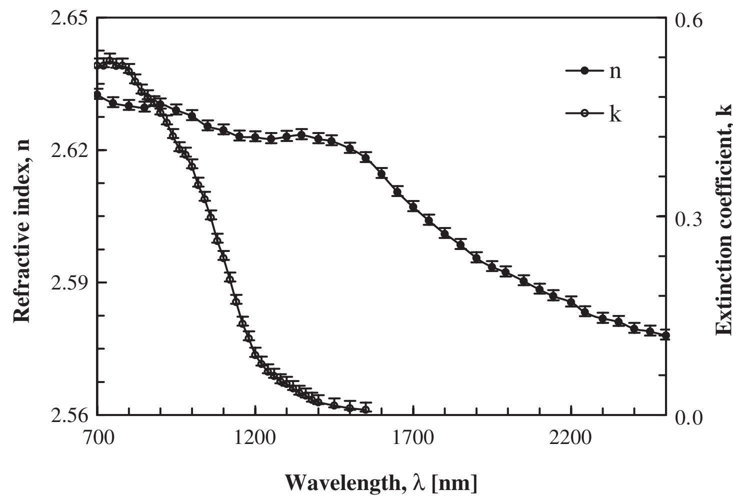

Figure 4. The refractive index, n, and extinction coefficient, k, for the deposited films.

Due to the higher refractive index of HgSe thin films it can be used as one of the layers in multi-layer antireflection coating or as a single layer coating to boost the reflectance of substrates having a lower refractive index.

According to the simple dispersion theory [15, 16], in the region of low absorption the index of refraction of a dielectric medium is given by:

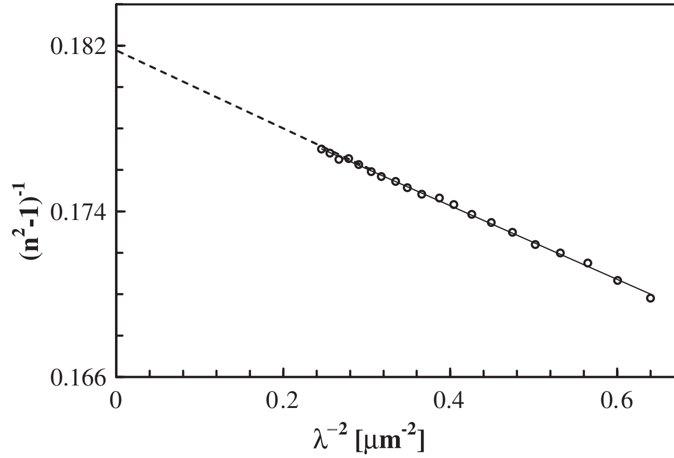

Figure 5. A plot of $(n^2 - 1)^{-1}$ versus λ^{-2}, in the near IR spectral region.

$$n^2(\omega) - 1 = \sum_i \left[\frac{f_i}{(\omega_i^2 - \omega^2)}\right]. \tag{4}$$

This equation separates the integrand optical transitions into individual dipole oscillators of frequency ω_i and strength f_i and can be rewritten in more conventional form in terms of wavelength, λ, as follows;

$$n^2(\lambda) - 1 = \sum_i \left\{\frac{S_i\lambda_i^2}{1 - (\frac{\lambda_i}{\lambda})^2}\right\} \tag{5}$$

where S_i is a strength factor. The index of refraction data is usually fitted to equation (5), known as the Sellmeier dispersion formula, using various long wavelength approximations. The most typical is to assume that one oscillator dominates and then to combine the other oscillators together into a constant A giving;

$$n^2(\lambda) - 1 = A + \frac{B\lambda^2}{\lambda^2 - C}. \tag{6}$$

This equation fits the dispersion of the refractive index quite well for most materials. However, the resulting curve fitting parameters, A, B, and C have no special physical significance. An excellent long wavelength approximation, which retains the physical significance of the oscillator parameters, is the single-term Sellmeier relation [17]

$$n^2(\lambda) - 1 = \frac{S_o\lambda_o^2}{\left[1 - (\frac{\lambda_o}{\lambda})^2\right]} \tag{7}$$

where λ_o is an average oscillator position and S_o is the average oscillator strength. S_o and λ_o are related directly to S_i and λ_i, and these in turn are connected to the energy band structure [17].

By plotting $(n^2 - 1)^{-1}$ versus λ^{-2} in the range 0.246–0.64 μm^{-2} (n is the average values for different films thicknesses), as shown in figure 5, and fitting a straight line to the infinite wavelength, one can estimate the values of $1/S_o$ and $1/\lambda_o S_o$ from the slope and intercept, respectively. The calculated S_o and λ_o values are 0.22×10^{14} m^{-2} and 0.49 μm, respectively. The dispersion parameter, E_o/S_o, where $E_o = \hbar c/e\lambda_o$ ($\hbar$, c, and e are the Planck constant, the speed of light, and electronic charge, respectively), is 2.87×10^{-13} eV m^2 for HgSe thin films. When these values of S_o and λ_o are substituted in equation (7), a plot of the refractive

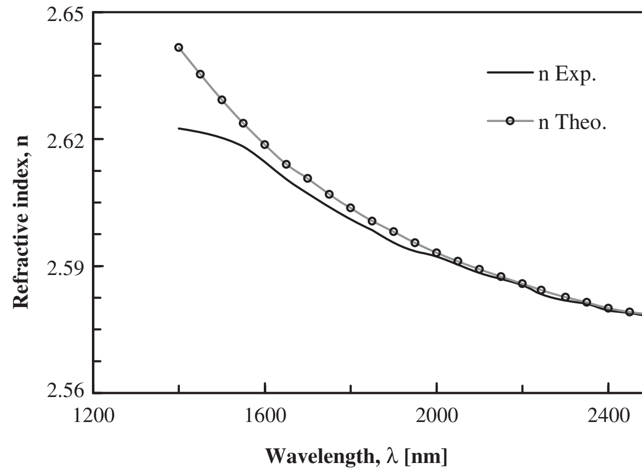

Figure 6. The experimental and theoretical refractive index, n, in the low absorption region.

index versus the wavelength is obtained and can be represented by a solid line as shown in figure 6 together with the experimental points. The good agreement between the experimental points and theoretically evaluated values in the transmission and low absorption region (1500–2500 nm) shows that the single oscillator model adequately describes the refractive index dispersion in the considered region.

The high frequency dielectric constant, ε_∞, of HgSe thin films could be determined from the spectral behaviour of the index of refraction. Two procedures have been followed. The first was to extrapolate the free carrier and lattice dispersion to infinite energy. This was performed by plotting n^2 versus λ^2 and extrapolating the long wavelength linear region to zero wavelength which yields $n_0^2 = \varepsilon_\infty$, as shown in figure 7. The second procedure was to assume that the high frequency properties of HgSe could be treated as a single oscillator at wavelength, λ_o, and apply the simple classical dispersion relation [18]. The values of ε_∞ obtained from the first and second procedures are 6.781 and 6.513, respectively. These values are compatible with the literature values of 7.5 ± 1 [19], 6.6 ± 0.5 [20], and 7.3 ± 0.3 [21].

Using the mean value of the extinction coefficient, k, the absorption coefficient α can be calculated. It was found that the absorption coefficient of HgSe thin films changes from 0.65×10^3 to 9.6×10^4 cm^{-1} in the photon energy range 0.8–1.44 eV. Analysis of the absorption coefficient gives information about the band structure of the material. Plotting $(\alpha\hbar\omega)^2$ versus photon energy ($\hbar\omega$) gave the straight line in figure 8, indicating an allowed direct transition described by [14, 16]:

$$(\alpha\hbar\omega) = A(\hbar\omega - E_g)^{1/2}. \tag{8}$$

The estimated direct band gap value $E_g = 0.84$ eV is consistent with that of 0.8 eV reported by Hankare *et al* [11]. The larger absorption coefficient of HgSe films ($\sim 10^4$ cm^{-1}) and the estimated optical band gap value make the material suitable for solar cell applications.

Furthermore, energetic electron beams are known to lose energy when passing through a thin film in electron energy-loss spectroscopy, with the amount of energy loss related to the free-electron density in the material. The surface, $-\text{Im}(1/\varepsilon)$, and volume, $-\text{Im}(1/(\varepsilon + 1))$, energy loss functions are related to the optical properties via the well known dielectric functions

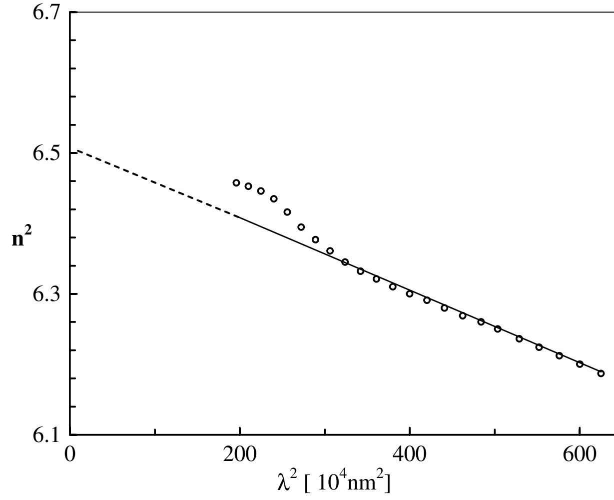

Figure 7. A plot of n^2 versus λ^2 in the near infrared region.

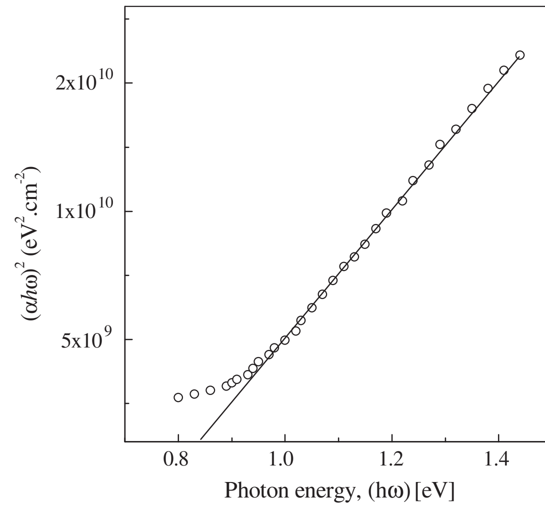

Figure 8. $(\alpha\hbar\omega)^2$ versus photon energy, $(\hbar\omega)$.

$\varepsilon_i = 2nk$ and $\varepsilon_r = n^2 - k^2$ by the following equations [22]:

$$-\mathrm{Im}\left(\frac{1}{\varepsilon^*}\right) = \frac{\varepsilon_i}{(\varepsilon_r^2 + \varepsilon_i^2)}$$
$$-\mathrm{Im}\left(\frac{1}{\varepsilon^* + 1}\right) = \frac{\varepsilon_i}{[(\varepsilon_r + 1)^2 + \varepsilon_i^2]}. \tag{9}$$

Figure 9 shows the graphical representation of the surface and energy-loss functions for HgSe thin films. It was found that both surface and volume energy loss increases with increasing photon energy.

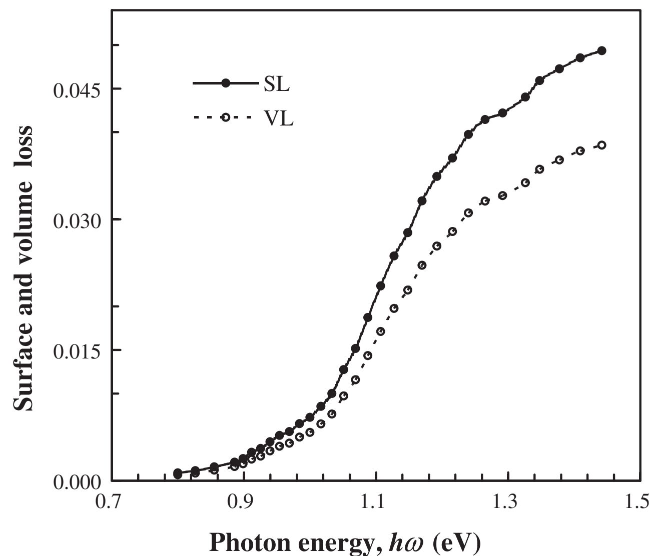

Figure 9. Graphical representation of both surface and volume energy loss functions against wavelength.

4. Conclusions

Good quality HgSe thin films have been successfully grown using the reactive solution process. The x-ray diffraction investigation revealed that both HgSe films as well as the precipitated powder are polycrystalline structures corresponding to cubic phase with a lattice constant 'a' = 0.6087 nm. The EDX investigation indicated that the as-grown films are nearly stoichiometric with chemical composition $Hg_{0.986}Se_{0.95}K_{0.064}$.

The transmittance and reflectance spectra of as-grown HgSe thin films were recorded at normal incidence of light in the wavelength range 700–2500 nm. The observed higher transmittance spectra (>85%) of HgSe films in the near infrared spectral region enables it to act as an efficient window material where more light can penetrate into the active region of the solar cells. The refractive index, n, and extinction coefficient, k, of the as-grown HgSe films have been determined using the transmittance and reflectance spectra. The refractive index n decreases with increasing wavelength and reaching a value of 2.578 at $\lambda = 2500$ nm. The higher refractive index suggests another possible use of HgSe thin films as antireflection coatings. The dispersion of the refractive index data was found to follow the simple dispersion theory, from which the average oscillator position, λ_o, average oscillator strength, S_o, and the high frequency dielectric constant, ε_∞, were calculated. Analysis of the optical absorption data of the as-grown films revealed an optical direct transition with band gap energy 0.84 eV. Graphical representation of the surface and volume energy loss functions indicated that both functions increase with increasing photon energy.

References

[1] Pejova B and Grozdanov I 2002 *Thin Solid Films* **408** 6
[2] Pejova B, Najdoski M, Grozdanov I and Dey S K 1999 *J. Mater. Chem.* **9** 2889
[3] Pejova B, Najdoski M, Grozdanov I and Dey S K 2000 *Mater. Lett.* **45** 269
[4] Salem A M and El-Gazzawi M E 2004 *Semicond. Sci. Technol.* **19** 236

[5] Salem A M and Abou-Helal M 2003 *Mater. Chem. Phys.* **80** 740
[6] Morales R L, Fafan M R, Moreno O P, Alvarez J P, Cabrera R H, Flores C A, Angel O Z, Mandujano O G, Angel P D, Montes J L M and Lopez L B 1999 *J. Electrochem. Soc.* **146** 2546
[7] Willardson R K and Beer A C 1981 *Semiconductors and Semimetals* vol 16 (New York: Academic)
[8] Singh K and Mishra S S D 1999 *J. Ind. Chem. Soc.* **76** 104
[9] Garadkar K M, Hankare P P and Patil R K 1999 *Mater. Chem. Phys.* **58** 64
[10] Hankare P P, Bhuse V M, Garadkar K M and Jadhav A D 2001 *Mater. Chem. Phys.* **71** 53–7
[11] Hankare P P, Bhuse V M, Garadkar K M, Delekar S D and Mulla I S 2003 *Mater. Chem. Phys.* **82** 711
[12] Delin A and Kluner T 2002 *Phys. Rev.* B **66** 035117
[13] Pramanik P and Bhattacharya S 1989 *Mater. Res. Bull.* **24** 945
[14] Pankove J I 1971 *Optical Process in Semiconductors* (New York: Dover)
[15] Born M and Wolf E 1970 *Principles of Optics* (Oxford: Pergamon)
[16] Moss T S, Burrell G J and Ellis B 1973 *Semiconductor Opto-Electronics* (London: Butterworths)
[17] DiDomenico M and Wemple S H 1969 *J. Appl. Phys.* **40** 720
[18] Wallmark J T 1959 *Proc. IRE* **45** 474
[19] Einfeldt S, Goschenhofer F, Becker C R and Landwehr G 1995 *Phys. Rev.* B **51** 4915
[20] Szuszkiewicz W 1979 *Phys. Status Solidi* b **91** 361
[21] Witowski A M and Grynberg M 1980 *Phys. Status Solidi* b **100** 389
[22] Salem A M 2002 *Appl. Phys.* A **74** 205